



Article

# Mettl3 Regulates Osteogenic Differentiation and Alternative Splicing of Vegfa in Bone Marrow Mesenchymal Stem Cells

Cheng Tian <sup>†</sup>, Yanlan Huang <sup>†</sup>, Qimeng Li , Zhihui Feng and Qiong Xu <sup>\*</sup>

Guanghua School of Stomatology & Guangdong Provincial Key Laboratory of Stomatology, Sun Yat-sen University, 56 Ling Yuan Xi Road, Guangzhou 510055, China; tianch5@mail2.sysu.edu.cn (C.T.); huangyanlan@mail2.sysu.edu.cn (Y.H.); liqimeng22@outlook.com (Q.L.); fzhh136@sina.com (Z.F.)

<sup>\*</sup> Correspondence: xqiong@mail.sysu.edu.cn; Tel.: +86-20-8387-0507; Fax: +86-20-8382-2807

<sup>†</sup> These authors are contributed equally to this study.

Received: 22 December 2018; Accepted: 25 January 2019; Published: 28 January 2019



**Abstract:** Bone mesenchymal stem cells (BMSCs) can be a useful cell resource for developing biological treatment strategies for bone repair and regeneration, and their therapeutic applications hinge on an understanding of their physiological characteristics. N<sup>6</sup>-methyl-adenosine (m<sup>6</sup>A) is the most prevalent internal chemical modification of mRNAs and has recently been reported to play important roles in cell lineage differentiation and development. However, little is known about the role of m<sup>6</sup>A modification in the cell differentiation of BMSCs. To address this issue, we investigated the expression of N<sup>6</sup>-adenosine methyltransferases (Mettl3 and Mettl14) and demethylases (Fto and Alkbh5) and found that Mettl3 was upregulated in BMSCs undergoing osteogenic induction. Furthermore, we knocked down *Mettl3* and demonstrated that *Mettl3* knockdown decreased the expression of bone formation-related genes, such as *Runx2* and *Osterix*. The alkaline phosphatase (ALP) activity and the formation of mineralized nodules also decreased after *Mettl3* knockdown. RNA sequencing analysis revealed that a vast number of genes affected by *Mettl3* knockdown were associated with osteogenic differentiation and bone mineralization. Kyoto encyclopedia of genes and genomes (KEGG) pathway analysis revealed that the phosphatidylinositol 3-kinase/AKT (PI3K-Akt) signaling pathway appeared to be one of the most enriched pathways, and Western blotting results showed that Akt phosphorylation was significantly reduced after *Mettl3* knockdown. Mettl3 has been reported to play an important role in regulating alternative splicing of mRNA in previous research. In this study, we found that *Mettl3* knockdown not only reduced the expression of *Vegfa* but also decreased the level of its splice variants, *vegfa-164* and *vegfa-188*, in *Mettl3*-deficient BMSCs. These findings might contribute to novel progress in understanding the role of epitranscriptomic regulation in the osteogenic differentiation of BMSCs and provide a promising perspective for new therapeutic strategies for bone regeneration.

**Keywords:** N6-methyladenosine; Mettl3; osteogenic differentiation; alternative splicing; Vegfa; PI3k-Akt

## 1. Introduction

N<sup>6</sup>-methyl-adenosine (m<sup>6</sup>A) is a methylation modification at the N6 position of adenosine in both coding and noncoding RNAs and has been identified as the most prevalent internal chemical modification of mRNAs in eukaryotes [1,2]. Although its presence was first described in the 1970s, the function of m<sup>6</sup>A remained a mystery until recently. The biological function and significance of m<sup>6</sup>A modification have recently begun to enter the limelight as a result of an m<sup>6</sup>A RNA immunoprecipitation approach followed by high-throughput sequencing [3]. m<sup>6</sup>A modifications are frequently found

near stop codons, at the beginning of 3' untranslated regions (3'UTRs) and within internal long exons [4,5]. All m<sup>6</sup>A sites are found within sequences conforming to the consensus sequence RR m<sup>6</sup>A CH([G/A/U][G>A] m<sup>6</sup>A C[U>A>C]) [6]. The m<sup>6</sup>A modification occurs by a methyltransferase complex, including methyltransferase-like 3 (METTL3), methyltransferase-like 14 (METTL14) and Wilms' tumor 1-associated protein (WTAP) in mammalian cells [7,8]. The modification is removed by fat-mass and obesity-associated protein (FTO) or  $\alpha$ -ketoglutarate-dependent dioxygenase alkB homolog 5 (ALKBH5) [9,10]. The addition of m<sup>6</sup>A affects different aspects of mRNA metabolism, such as RNA stability, translation, alternative polyadenylation and pre-mRNA splicing [9,11,12]. Previous studies have demonstrated that m<sup>6</sup>A methylation has a profound effect on cell differentiation, embryonic development and stress responses [13–15].

Mesenchymal stem cells (MSCs) are a heterogeneous population of stem cells that can be harvested from many different sources and differentiate into mesoderm-type lineages, including osteoblasts, chondrocytes, and adipocytes [16–19]. MSCs have been widely used in stem cell transplantation, gene therapy, tissue engineering, and immunotherapy [20–22]. Bone mesenchymal stem cells (BMSCs) are commonly isolated and characterized from bone marrow aspirates and have been extensively investigated as the most promising cellular source for bone regeneration for both research and clinical purposes [23–28]. Numerous studies have demonstrated the beneficial effects of BMSCs on bone regeneration and repair, including stimulation of their differentiation into osteoblasts, stimulation of angiogenesis, immunomodulatory effects, antiapoptotic effects on osteogenic lineage cells, and recruitment of host MSCs/progenitor cells [29–35]. BMSCs have high affinity to differentiate into osteogenic lineages, and their differentiation into osteoblast cells is a pivotal step during bone regeneration and repair [36–42].

Bone reconstruction is a complex process of overlapping phases, including inflammation, repair, and remodeling, and involves many intracellular signaling pathways and growth factors [43–46]. Multiple signaling pathways have been reported to be involved in the osteogenic differentiation of BMSCs, such as bone morphogenetic protein (BMP)-Smad pathways, Wnt/ $\beta$ -catenin pathways, and PI3K-Akt pathways [47–51]. Osteogenesis and angiogenesis are highly coupled in the process of bone formation, and angiogenesis is a prerequisite step for bone tissue regeneration [52–54]. In tissue-engineered bone, BMSCs not only directly differentiate into endothelial cells to participate in new blood vessel formation in the bone defect area but also secrete angiogenic factors, such as vascular endothelial growth factor (VEGF) and angiopoietin, to promote local angiogenesis. As one of the most potent inducers of angiogenesis, VEGF is particularly intriguing due to its dual role in bone and endothelial development and plays an important role in bone formation [55,56]. Previous studies have shown that VEGF has been successfully used for enhanced bone regeneration due to its capacity to promote both osteogenic and angiogenic differentiation [57,58]. The angiogenic activity of BMSCs has been suggested to contribute to their regenerative capability.

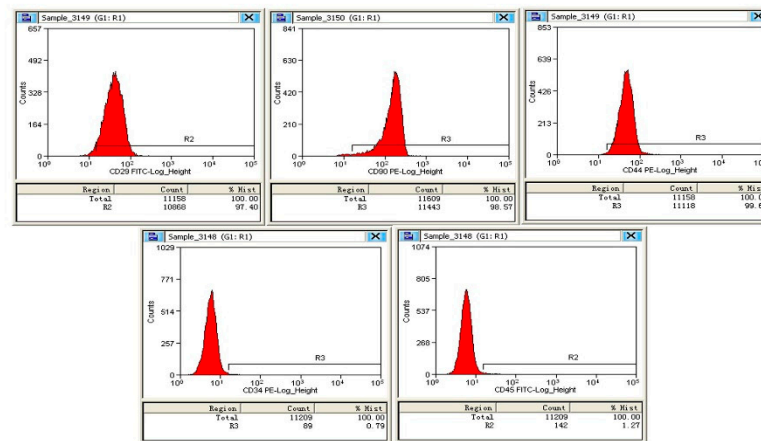
While much evidence has demonstrated that the osteogenic differentiation of BMSCs is intimately associated with multiple genetic factors, such as signaling molecules and growth factors, the epigenetic regulatory mechanisms underlying cell differentiation have attracted increasing attention [59–61]. Recent evidence has illustrated that epigenetic modifications, such as histone acetylation and DNA methylation, are involved in the cell differentiation process of BMSCs during bone regeneration [62,63]. As another layer of epigenetic regulation (RNA epigenetics), m<sup>6</sup>A modification has recently been reported to play important roles in cell function and the differentiation of embryonic stem cells (ESCs) and various cancer cell types [64–66]. However, little is known about the role of m<sup>6</sup>A modification in the cell differentiation of BMSCs. Whether m<sup>6</sup>A affects the angiogenic factor Vegf during the osteogenic differentiation process of BMSCs also remains to be determined. Therefore, the aims of this study were to investigate the effect of m<sup>6</sup>A methylation on the osteogenic differentiation of BMSCs and to determine its role in regulating Vegf.

## 2. Results

### 2.1. Selection and Identification of BMSCs

To confirm the type of the separated BMSCs, third-passage cells were identified by flow cytometry to recognize the surface markers. The results showed expression of CD29+, CD44+, CD90+, CD34–, and CD45– (Figure 1A,B), indicating that the BMSCs were of high purity. Moreover, the BMSCs were able to be differentiated into osteoblast-like cells and adipose-like cell when cultured in differentiating induction medium, as determined by Alizarin Red S staining and Oil Red O staining, respectively (Figure 1C–E). These data confirmed the status of the isolated and cultured BMSCs.

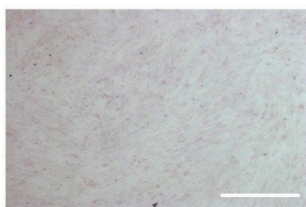
**A**



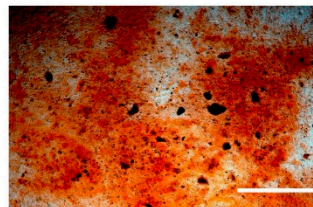
**B**

Surface markers	Percentage ( Mean%±S.D.)
CD29+	97.40±1.20
CD90+	98.57±0.83
CD44+	99.64±0.97
CD34-	0.79±0.67
CD45-	1.27±0.76

**C**



**D**



**E**

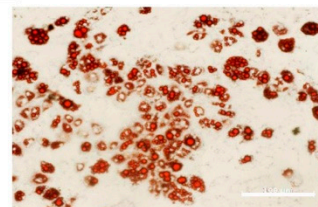


**Figure 1.** Characterization of BMSCs. (A) The expression of cell surface markers was evaluated by flow cytometry. Average of cells (%) are shown in (B) as Mean% ± S.D. (standard deviation). (C–E) The differentiation ability of BMSCs towards osteogenesis-like or adipogenesis-like cells was assessed by Alizarin Red S staining (D) or Oil Red O staining (E). The “white” scale bars represent 100 μm (original magnification ×100).

## 2.2. Expression of *m*<sup>6</sup>A Methyltransferase and Demethylases in BMSCs Undergoing Osteogenic Differentiation

During the osteogenic differentiation of BMSCs, cells were cultured in osteogenic induction medium at the indicated time points, and alkaline phosphatase (ALP) activity and mineralized nodule formation were estimated after induction. As shown in Figure 2C, cells cultured with osteogenic induction medium displayed significantly higher ALP activity on Day 7 than on Day 0. Mineralized matrix deposition was higher after 21 days of osteogenic induction than after 0, 7, and 14 days (Figure 2A,B). The expression levels of several osteogenic markers were also upregulated, as shown by quantitative real time polymerase chain reaction (qRT-PCR) and Western blotting, further confirming the osteogenic differentiation of BMSCs (Figure 2D,E).

To investigate the role of *m*<sup>6</sup>A modification in the osteogenic differentiation potential of BMSCs, the expression patterns of an *m*<sup>6</sup>A methyltransferase (Mettl3) and demethylases (Fto, Alkbh5) were measured during the osteogenic induction of BMSCs. Both the mRNA and protein levels of Mettl3 increased after 7 and 14 days of osteogenic induction (Figure 2F,G). Although *Fto* increased at the mRNA level after 7 and 14 days, its protein level showed no significant difference. *Alkbh5* showed no significant difference at either the mRNA or protein level. Accordingly, the expression pattern of Mettl3 during osteogenic differentiation was consistent with those of the mineralization-related markers.

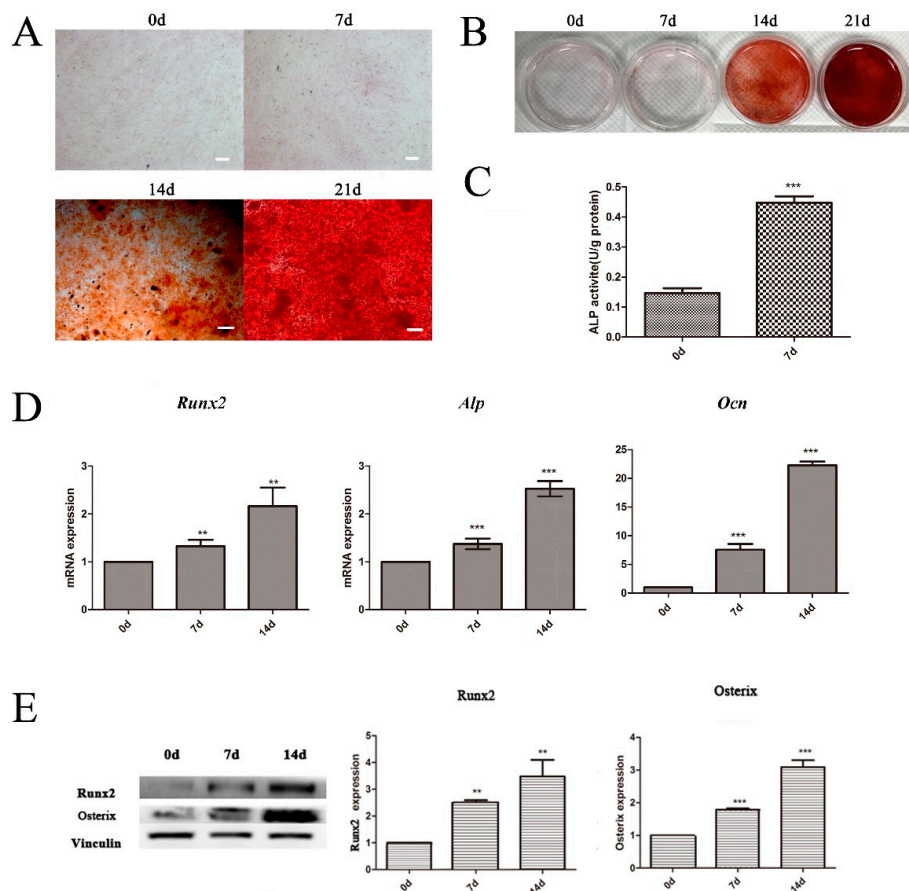
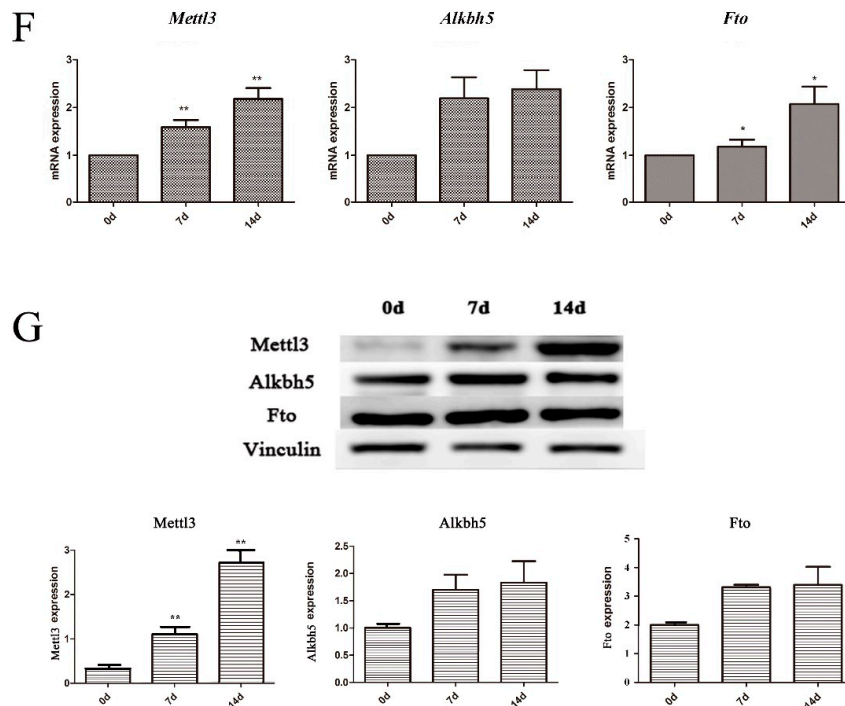


Figure 2. Cont.



**Figure 2.** Osteogenic differentiation of BMSCs and expression of m<sup>6</sup>A methyltransferase and demethylases. (A,B) The formation of mineralized nodules was analyzed in BMSCs undergoing osteogenic differentiation on Days 7, 14, and 21. The “white” scale bars represent 100  $\mu$ m (original magnification  $\times$ 100). (C) ALP activity assays. ALP activity was significantly higher in the cells cultured in osteogenic differentiation medium for seven days. (D) The expression of *Runx2*, *Alp* and *Ocn* was assessed using qRT-PCR on Days 7 and 14 of culture in osteogenic induction medium. *Gapdh* was used as an internal control. (E) The expression of *Runx2* and *Osterix* was examined using Western blotting. Vinculin was used as an internal control. The band intensities were analyzed using ImageJ software. (F,G) RNA methylation modification-related enzymes were detected using qRT-PCR and Western blotting in cells cultured in osteogenic induction medium for 7 and 14 days. *Gapdh* was used as an internal control for qRT-PCR. Vinculin was used as an internal control in Western blotting. All of the results represent the mean  $\pm$  standard deviation of three independent experiments ( $n = 3$ ). Significant difference compared with the control (\*  $p < 0.05$ ; \*\*  $p < 0.01$ ; \*\*\*  $p < 0.001$ ).

### 2.3. Effect of *Mettl3* Knockdown on the Osteogenic Differentiation Potential of BMSCs

To explore the function of *Mettl3* in the osteogenic differentiation process of BMSCs, specific shRNAs were applied to knock down its expression in BMSCs. Quantification of lentiviral gene transfer efficiency in BMSCs was measured via the proportion of fluorocytes. A transfer efficiency up to 90% was achieved at 48 h after transfection (Figure 3A). The *Mettl3* protein level exhibited an approximate 60% decrease in the shRNA group (#sh1) compared with the negative control group, suggesting that *Mettl3* was effectively silenced in BMSCs (Figure 3B). *Mettl3*-sh1 was thus chosen for further experiments.

To investigate the differentiation potential of BMSCs after *Mettl3* knockdown, the expression levels of several osteogenic markers were measured. The results showed that *Mettl3* knockdown reduced the mRNA levels of *Alp* and *Ocn* in BMSCs after osteogenic differentiation induction for 7 and 14 days (Figure 3C). The mRNA and protein expression of *Runx2* and *Osterix* also decreased in *Mettl3*-shRNA cells (Figure 3D).

To verify the effect of *Mettl3* knockdown on the mineralization potential of BMSCs, ALP activity and the formation of mineralized nodules were then examined in *Mettl3*-shRNA cells. ALP activity decreased on Day 7, and the formation of mineralized nodules was reduced on Days 7, 14, and 21 after osteogenesis induction (Figure 3E,F).

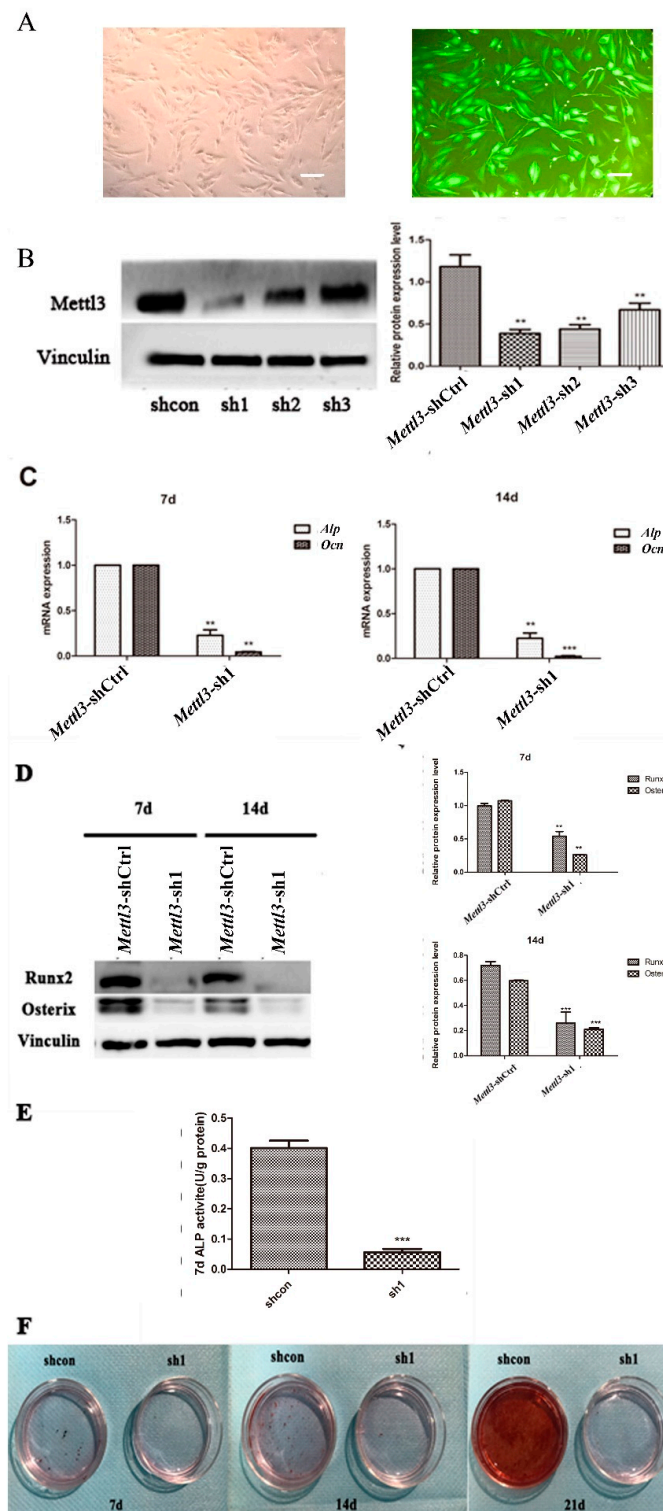


**Figure 3.** Effect of *Mettl3* knockdown on the osteogenic differentiation potential of BMSCs. (A) A green fluorescence protein marker was used to determine the transfer efficiency of *Mettl3* knockdown in BMSCs. After transfection for 72 h, the cells were observed under a microscope (on the left). The right image is an immunofluorescence image taken at the same time. The “black” scale bars represent 100  $\mu$ m (original magnification  $\times 100$ ). (B) The expression level of *Mettl3* was determined using Western blotting in the *Mettl3*-shRNA and *Mettl3*-shCtrl groups. Vinculin was used as an internal control. The band intensities were analyzed using ImageJ software. (C) The mRNA expression levels of *Alp* and

*Ocn* in the *Mettl3*-shRNA and *Mettl3*-shCtrl groups were assessed using qRT-PCR after 7 and 14 days of osteogenic induction. *Gapdh* was used as an internal control. (D) The protein levels of Runx2 and Osterix in the *Mettl3*-shRNA and *Mettl3*-shCtrl groups were assessed using Western blotting after 7 and 14 days of osteogenic induction. Vinculin was used as an internal control. The band intensities were analyzed using ImageJ software. (E) ALP activity was determined in *Mettl3*-shRNA and *Mettl3*-shCtrl cells cultured in osteogenic differentiation medium for seven days. (F) The formation of mineralized nodules was analyzed in the *Mettl3*-shCtrl and *Mettl3*-shRNA groups undergoing osteogenic induction on Days 7, 14, and 21. Mineralization was analyzed using Alizarin Red S staining. All of the results represent the mean  $\pm$  standard deviation of three independent experiments ( $n = 3$ ). Significant difference compared with the control (\*  $p < 0.05$ ; \*\*  $p < 0.01$ ; \*\*\*  $p < 0.001$ ).

#### 2.4. Differentially Expressed Genes in *Mettl3*-Knockdown BMSCs

To further determine the effect of *Mettl3* on the differentiation of BMSCs, *Mettl3*-shRNA and *Mettl3*-shCtrl cells undergoing osteogenic induction for 14 days were subjected to RNA sequencing. The genes that were differentially expressed following *Mettl3* knockdown with a Log2 ratio  $>2$  or  $<-2$  were revealed in the heat map (Figure 4A). Among these genes, 556 genes were upregulated and 641 genes were downregulated (Figure 4B). Furthermore, gene ontology (GO) enrichment and KEGG pathway analyses were utilized to cluster the biological processes and pathways that were differentially inhibited between sh*Mettl3* and shCtrl cells. In the biological process analysis of genes downregulated by *Mettl3* knockdown with a Log2 ratio  $<-2$ , the significant GO terms were related to ossification, cell adhesion, bone mineralization, and positive regulation of cytosolic calcium ion concentration (Figure 4C). From KEGG pathway analysis of the genes downregulated by *Mettl3* knockdown, the top ten enriched pathways were shown in Figure 4D. Among the signaling pathways that are closely related to osteogenic differentiation, the phosphatidylinositol 3-kinase (PI3K)-Akt signaling pathway appeared to be one of the most enriched pathways.

To confirm the inhibition of the PI3K-Akt pathway following *Mettl3* knockdown in BMSCs, Western blotting was performed to evaluate the phosphorylation level of Akt. Compared to the control group, the group with *Mettl3* knockdown exhibited a significant decrease in Akt phosphorylation (Figure 4E), indicating that PI3K-Akt signaling was suppressed by *Mettl3* knockdown in BMSCs during the osteogenic differentiation process.

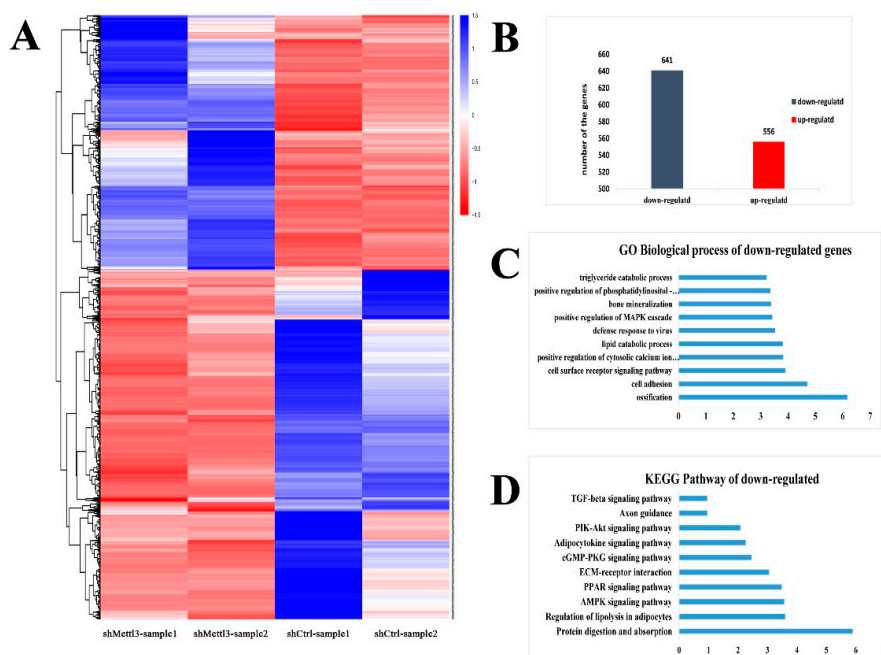
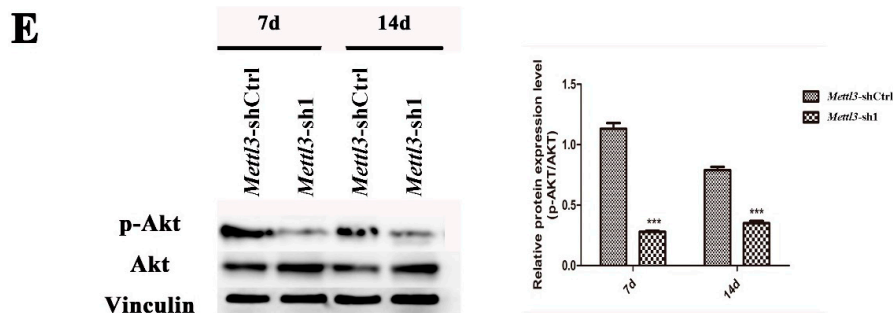


Figure 4. Cont.



**Figure 4.** Differential expression of mRNAs between *Mettl3*-knockdown and control. (A) The differentially expressed genes in *Mettl3*-knockdown BMSCs under osteogenic induction medium are shown in the heat map. A  $p$  value cut-off of 0.05 and a  $\text{Log}_2$  ratio  $>2$  or  $<-2$  were used as a filter to identify the differentially expressed genes. (B) The differentially expressed genes were counted; among these genes, 556 were upregulated and 641 were downregulated. (C,D) GO and KEGG pathway analyses of genes that were differentially expressed with a  $\text{Log}_2$  ratio  $<-2$ , ordered according to gene enrichment. (E) The expression levels of total Akt and activated Akt (P-Akt) were assessed using Western blotting. Vinculin was used as an internal control. The band intensities were analyzed using ImageJ software. All of the results represent the mean  $\pm$  standard deviation of three independent experiments ( $n = 3$ ). Significant difference compared with the control (\*\*\*)  $p < 0.001$ .

### 2.5. Effect of *Mettl3* Knockdown on the Expression of *Vegfa* and Its Splice Variants

The angiogenic factor VEGF is closely related to the osteogenic differentiation potential of BMSCs. The *Vegfa* expression in *Mettl3*-knockdown BMSCs was detected, and the results showed that *Mettl3* knockdown decreased the expression level of *Vegfa* during the osteogenic differentiation of BMSCs (Figure 5B).

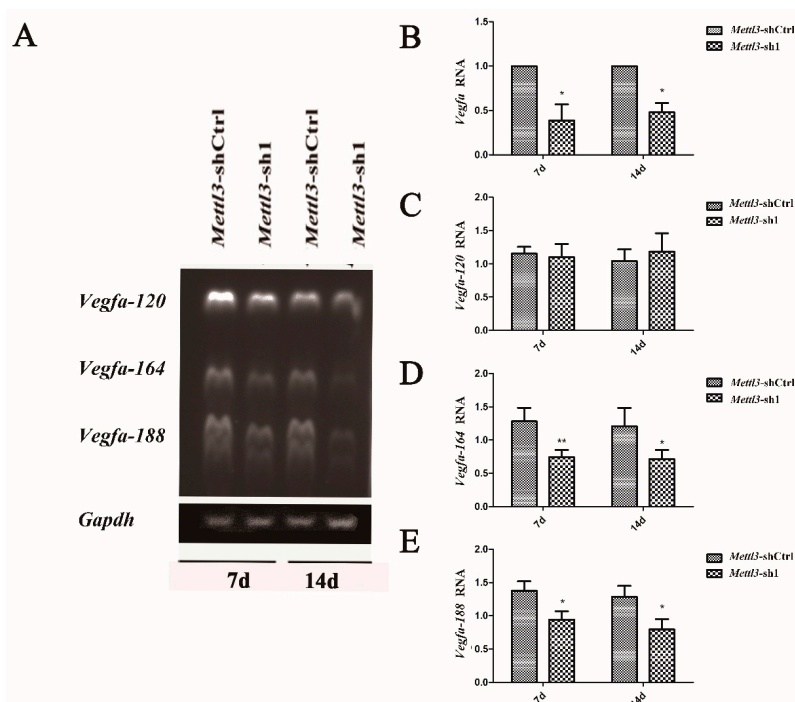


**Figure 5.** Effect of *Mettl3* knockdown on the mRNA expression of *Vegfa* and its splice variants. (A) RT-PCR was performed to amplify mRNA products specific to *Vegfa* isoforms or an mRNA product specific to *Gapdh*. (B) The expression of *Vegfa* was decreased after *Mettl3* knockdown, as indicated by the qRT-PCR results. (C–E) The mRNA expression of *Vegfa* isoforms was assessed with the expected mRNA sizes of 431 bp for *Vegfa-120*, 563 bp for *Vegfa-164*, and 635 bp for *Vegfa-188*. *Gapdh* was used as an internal control for qRT-PCR and RT-PCR. The data are presented as the mean  $\pm$  standard deviation of three independent experiments ( $n = 3$ ). Statistically significant difference relative to the shCtrl group (\*  $p < 0.05$ ; \*\*  $p < 0.01$ ).

Alternative splicing is the most common event in transcript isoforms. [67,68] *Mettl3* has been reported to play an important role in regulating alternative splicing of mRNA [69–71]. Previous studies reported that the alternative splicing of *Vegfa* affects the osteogenic differentiation of BMSCs [72,73]. *Vegfa* contains three homologous splice variants: *Vegfa-120*, *Vegfa-164*, and *Vegfa-188* [74]. To analyze whether *Vegfa* and its alternative splicing are modulated by *Mettl3* in BMSCs undergoing osteogenic differentiation, we performed RT-PCR to detect three *Vegfa* isoforms. The results indicated that *Mettl3* knockdown decreased the mRNA expression of *Vegfa-164* and *Vegfa-188* but did not significantly alter *Vegfa-120* mRNA level (Figure 5A,C–E).

### 3. Discussion

m<sup>6</sup>A is a prevalent epitranscriptomic modification in mRNAs and is widely conserved across single-cell organisms, plants and vertebrates [75–77]. m<sup>6</sup>A methylation occurs during nascent pre-mRNA processing by a methyltransferase complex consisting of METTL3, METTL14, and WTAP and is removed by FTO and ALKBH5 [9]. This modification has been shown to regulate the pluripotency and differentiation of ESCs and somatic cell reprogramming. m<sup>6</sup>A methylation on some transcripts in ESCs, particularly those encoding developmental regulators, blocks HuR binding and maintains ESC self-renewal capability [78]. Depletion of m<sup>6</sup>A in the mRNA of *Mettl3*<sup>-/-</sup> ESCs limits naïve marker priming and differentiation competence, which leads to a “hyper”-naïve pluripotency phenotype [79]. Overexpression of *Mettl3* in mouse embryonic fibroblasts (MEFs) increases m<sup>6</sup>A levels and significantly increases the reprogramming efficiency by enhancing the expression of key pluripotent factors [80].

BMSCs are the most suitable and widely used progenitor cell population for bone regeneration due to their capacity for multilineage differentiation and the potential to increase osteoinduction and osteogenesis [19,22]. BMSCs are known to stimulate bone tissue regeneration, but the mechanism by which the effect occurs has not yet been elucidated. To explore the role of m<sup>6</sup>A-dependent RNA methylation in the osteogenic differentiation of BMSCs, BMSCs were cultured using osteogenic induction medium to establish an osteogenesis model. The expression levels of main m<sup>6</sup>A methyltransferase and demethylases, including *Mettl3*, *Fto* and *Alkbh5*, were then evaluated. The results showed that *Mettl3* mRNA and protein levels increased after osteogenic induction, but the protein expression of *Fto* and *Alkbh5* levels did not significantly differ with or without osteogenic differentiation. These findings indicated that *Mettl3*-dependent RNA methylation might be involved in the osteogenic differentiation of BMSCs.

METTL3 (also known as MTA70) is identified as the main methyltransferase critical for m<sup>6</sup>A methylation [81,82]. Deletion or overexpression of *METTL3* changes the total m<sup>6</sup>A methylation level, which has a direct effect on cell survival, stem cell maintenance, and lineage determination [83–85]. Depletion of the *Mettl3* homolog in *Arabidopsis thaliana* gives rise to plants with altered growth patterns and reduced apical dominance [86]. The inhibition of the *Drosophila* *Mettl3* homolog (*Dm ime4*) has been proven to inhibit oogenesis [87]. *METTL3* inhibition leads to a concomitant decrease in the cellular m<sup>6</sup>A level and apoptosis of human HeLa cells [88]. To elucidate the role of *Mettl3* in the osteogenic differentiation of BMSCs, *Mettl3* was silenced in BMSCs, and the effect of *Mettl3* knockdown on cell differentiation was investigated in the present study. The results showed that *Mettl3* knockdown reduced the accumulation of osteogenic differentiation markers such as *Runx2* and *Osterix*. The ALP activity and the formation of mineralized nodules were also decreased after *Mettl3* knockdown. Differentially expressed genes in *Mettl3* knockdown cells were subjected to RNA sequencing, and the results suggested that many genes were regulated by *Mettl3* knockdown. GO term analysis indicated that downregulated genes were associated with ossification, cell adhesion, and bone mineralization. KEGG pathway analysis revealed that the signaling pathways associated with the downregulated genes, such as PI3K-Akt signaling pathway, AMPK signaling pathway, and PPAR signaling pathway, were mostly involved in protein digestion and absorption, regulation of lipolysis in adipocytes, and osteogenic differentiation. Among the signaling pathways that are closely

relevant to the osteogenic differentiation, the PI3K-Akt signaling pathway appeared to be one of the most enriched pathways. The PI3K-Akt signaling pathway is known to play a regulatory role in the survival, proliferation, migration, and differentiation of rabbit and human MSCs [89,90]. PI3K-Akt signaling also acts as a crucial regulator in bone tissue metabolism and the osteogenic differentiation of BMSCs [91]. Our Western blotting results confirmed a significant reduction in Akt phosphorylation after *Mettl3* knockdown, which was consistent with the RNA sequencing results. The above data suggested that *Mettl3* increases the osteogenic differentiation of BMSCs.

Reconstructing local microcirculation and increasing blood vessel density are essential changes for effective bone regeneration [41,92–95]. VEGF is the most attractive and well-characterized factor for the therapeutic induction of new blood vessel growth. VEGF can be secreted by different MSC populations in a paracrine manner and influences endothelial cell behavior [57,58]. This growth factor is not only involved in angiogenesis but is also implicated in the maturation of osteoblasts, ossification, and bone turnover. Therefore, VEGF is widely used to induce angiogenesis and osteogenesis in bone tissue engineering constructs [96–98]. In rodents, *Vegfa* contains three homologous splice variants: 120, 164, and 188 amino acids [74]. *Vegfa-120*, the shortest variant, is less effective in promoting MSC growth. *Vegfa-164* plays a regulatory role in improving MSC proliferation and chondrogenic differentiation, and *Vegfa-188* is more effective in promoting the osteogenic differentiation of MSCs [99]. The present study indicated that *Mettl3* inhibition decreased the expression level of *Vegfa* during the osteogenic differentiation of BMSCs. The low expression of *Vegfa* might inhibit the osteogenic differentiation of BMSCs in turn. *Mettl3* localizes predominantly in nuclear speckles, which are sites of mRNA splicing and storage [100]. Several studies have implied that *Mettl3* plays an important role in regulating alternative splicing of mRNA [69–71]. To clarify whether *Mettl3* affects the alternative splicing pattern of *Vegfa*, the expression levels of *Vegfa* variants were determined using RT-PCR in *Mettl3*-depleted BMSCs. The results demonstrated that *Mettl3* knockdown did not significantly alter *Vegfa-120* mRNA level but significantly decreased the mRNA levels of *Vegfa-164* and *Vegfa-188*, which are related to MSC proliferation and differentiation. These findings indicated that *Mettl3* knockdown limited the expression of *Vegfa* and its bone formation-related splice variants in osteoblast-induced BMSCs.

In conclusion, the present study estimated the expression pattern of m<sup>6</sup>A methyltransferase and demethylases during the osteogenic differentiation of BMSCs and demonstrated that *Mettl3* is highly expressed in osteogenically differentiated BMSCs. Investigating the role of *Mettl3* in regulating cell differentiation showed that the loss of *Mettl3* suppressed the osteogenic differentiation potential of BMSCs. *Mettl3* knockdown also decreased the expression of *Vegfa* and its splice variants in BMSCs. These findings might contribute to novel progress in the role of the epitranscriptome in osteogenic differentiation and provide a promising perspective for the development of innovative therapeutic strategies for bone regeneration.

## 4. Materials and Methods

### 4.1. Cell Culture and Osteogenic Differentiation

BMSCs were obtained from the femurs and tibias of 2–3-week-old Sprague-Dawley male rats (Animal Center of Sun Yat-sen University) as described previously by Liu et al. [101]. BMSCs were seeded in 25-cm<sup>2</sup> culture flasks and were maintained by Dulbecco's Modified Eagle Medium: Nutrient Mixture F-12 (DMEM/F12, Gibco, Grand Island, NY, USA) supplemented with 10% fetal bovine serum (FBS; Gibco, Grand Island, NY, USA) and 1% penicillin/streptomycin (Invitrogen, Carlsbad, NM, USA). The medium was renewed every 3 days. When reaching 90% confluence, BMSCs were harvested using trypsin/EDTA (Gibco, Grand Island, NY, USA) and reseeded into dishes (10 cm in diameter). The expression levels of different cell surface markers, including CD29+, CD44+, CD90+, CD34– and CD45–, were determined by flow cytometry. Cells from the third passage were used in further experiments.

For osteogenic differentiation, BMSCs were cultured using osteogenic induction medium, which contained DMEM/F12 supplemented with 100 nmol/L dexamethasone, 50 g/L ascorbic acid and 10 nmol/L  $\beta$ -glycerophosphate (Sigma-Aldrich, St. Louis, MO, USA) for 7 and 14 days. Cells without osteogenic induction medium were used as the control.

#### 4.2. *Mettl3* Knockdown Using shRNA Transfection

Short hairpin RNA (shRNA) against *Mettl3* shRNA: AGTCACAAACCAGATGAAATA and a nonspecific shRNA construct were designed and cloned into a hU6-MCS-Ubiquitin-EGFP-IRES-puromycin vector. The recombinant lentiviral vector was transfected into 293FT cells. The supernatant was harvested after 48 h and transduced into BMSCs. The cells were then incubated in solution with 1  $\mu$ g/mL puromycin (Sigma-Aldrich, St. Louis, MO, USA) for 2 weeks. The stable clones were then maintained in 0.5  $\mu$ g/mL puromycin and were observed and counted with a fluorescence microscope to ensure that the transfection rate was over 90%, and the knockdown effect was confirmed using a Western blotting assay. The cells were independently divided into 3 groups: control (untransduced group), shCtrl (negative control group), and shMettl3.

#### 4.3. Western Blot Analysis

The BMSCs were harvested using RIPA lysis buffer (Cell Signaling Technology, Boston, MA, USA) containing protease inhibitor cocktail (Cwbiotech, Beijing, China). Forty micrograms of protein were electrophoresed in 10% sodium dodecyl sulfate polyacrylamide gel electrophoresis and then transferred onto polyvinylidene fluoride membranes (PVDF) (Millipore, Billerica, MA, USA) in transfer buffer with 10% methanol. The membrane was blocked in TBST containing 5% nonfat milk for 1 h at room temperature and then incubated with the following primary antibodies overnight at 4 °C: *Mettl3* (1:1000; Proteintech, Chicago, IL, USA), *Fto* (1:1000; Abcam, Cambridge, UK), *Alkbh5* (1:1000; Proteintech, Chicago, IL, USA), *Runx2* (1:1000; Abcam, Cambridge, UK), *Osterix* (1:1000; Abcam, Cambridge, UK), *Akt* and *P-Akt* (1:1000; Cell Signaling Technology, Boston, MA, USA), *Gapdh* (1:1000; Abcam, Cambridge, UK), and *Vinculin* (1:1000; Cell Signaling Technology, Boston, MA, USA). The membrane was then incubated with secondary antibodies (Abcam, Cambridge, UK) for 1 h at room temperature after washing. The blot showing antibody binding was developed with an enhanced chemiluminescence system (Millipore, Billerica, MA, USA) and captured via an ImageQuant LAS 4000 mini system (GE Healthcare Life Sciences, Illinois, NJ, USA). Band densities were quantified using ImageJ v1.47 software (National Institutes of Health, Bethesda, MD, USA).

#### 4.4. Alizarin Red S Staining

To detect mineralized nodule formation, BMSCs seeded in 6-well plates were induced in osteogenic medium for 0, 7, and 14 days. After culturing, the cells were rinsed with PBS and fixed in 4% paraformaldehyde solution for 20 min, stained with 1% Alizarin Red S (GL Biochem, Shanghai, China) solution at room temperature for 10 min, and washed 5 times. Mineralized nodules were then photographed under an inverted phase contrast microscope (Axiovert 40; Zeiss, Jena, Germany).

#### 4.5. Alkaline Phosphatase Activity Assay

Cells seeded in 24-well plates were cultured in osteogenic differentiation medium for 7 days. Alkaline phosphatase activity was determined utilizing an ALP assay kit (Nanjing Jiancheng Bioengineering Institute, Nanjing, China). Cells were lysed with 1% Triton X-100 for 30 min at 4 °C. The optical density (OD) value of the solution was quantified by measuring the absorbance at 520 nm by a microplate reader (Tecan, Hombrechtikon, Switzerland). The protein content was examined by a bicinchoninic acid protein assay (Beyotime Biotechnology, Haimen, China), and ALPase levels were standardized to the total protein concentration.

#### 4.6. Quantitative Real-Time PCR (qPCR) and Reverse Transcription PCR (RT-PCR) Monitoring of mRNA Levels

Total RNA from BMSCs was extracted using TRIzol reagent (Invitrogen, Carlsbad, NM, USA). RNA samples were reverse-transcribed for cDNA synthesis using Superscript III Reverse Transcriptase (Invitrogen, Carlsbad, NM, USA). Subsequently, cDNA was used in PCR. PCR was performed and monitored using the Light Cycler 480. Samples were analyzed using primers listed in Table 1.

**Table 1.** Primers Used for the Analysis of mRNA Levels by qRT-PCR and RT-PCR.

Gene	Forward Primer	Reverse Primer
<i>Ocn</i>	5' ATCCATGCAGGCATCTCACC 3'	5' ACCTAACCAATTGCCCCCAG 3'
<i>Alp</i>	5' TCGATGGCTTTGGTACGGAG 3'	5' TCGGGGACATAAGCGAGTTT 3'
<i>Runx2</i>	5' GGCCAGGTTCAACGATCTGA 3'	5' GGACCGTCCACTGTCACTTTA 3'
<i>Mettl3</i>	5' CTTAGCATCTGGTCTGGGCT 3'	5' CCTTCTGCTCTGCTGTTCCCT 3'
<i>Alkbh5</i>	5' ACCACCAAACGGAAGTACCAG 3'	5' TCATCCTGGCTGAAGAGACG 3'
<i>Fto</i>	5' ACTGGTTTTCCGAGAGGCTG 3'	5' GTGAGCACGTCTTTCCTTG 3'
<i>Vegfa</i>	5' CTGCTCTCTGGGTGCACTGG 3'	5' CACCGCCTGGCTTGTCACAT 3'

To determine the expression of Vegfa splice variants, semiquantitative RT-PCR followed by agarose gel electrophoresis was performed. The pair of primers generated a different sized product for each of the splicing forms of VEGF mRNA. The predicted PCR products for the major forms, Vegf-120, Vegf-164, and Vegf-188 were 431, 563, and 635 bp, respectively [102]. One microgram of RNA was prepared and subjected to reverse transcription as described above. Reverse-transcribed cDNA was used for PCR using Taq DNA polymerase (Invitrogen, Carlsbad, NM, USA). PCR products were electrophoresed using 1.5% agarose gels, and images were captured using the FluorChem™ Q system (Alpha Innotech, San Jose, CA, USA).

#### 4.7. RNA Sequencing

Approximately 20 ng of Poly (A) RNA were purified from total RNA and converted to cDNA. The cDNA samples were sequenced with a HiSeq 2000 system (Illumina Inc., San Diego, CA, USA). The expression of transcripts was quantified as reads per kilobase per million reads (RPKM). Genes were considered differentially expressed genes when the expression showed twofold changes using RPKM. Gene Ontology (GO) and Kyoto Encyclopedia of Genes and Genomes (KEGG) analyses were performed with the Database for Annotation, Visualization and Integrated Discovery (DAVID: <http://david.abcc.ncifcrf.gov/>) to identify the significantly enriched pathways.

#### 4.8. Statistical Analyses

All experiments were performed at least in triplicate. The data are shown as the mean  $\pm$  standard deviation and were analyzed using the SPSS 20.0 software program (SPSS, Chicago, IL, USA). One-way analysis of variance was applied to compare the experimental groups. Differences were considered statistically significant differences for  $p < 0.05$ .

**Author Contributions:** C.T. and Q.X. conceived and designed the experiments; C.T. and Y.H. performed the experiments; Q.L. and Z.F. analyzed the data; Q.X. contributed the reagents; and C.T. wrote the paper.

**Funding:** This work was financially supported by the National Natural Science Foundation of China (81771058).

**Conflicts of Interest:** The authors deny any conflicts of interest.

## Abbreviations

BMSCs	Bone mesenchymal stem cells
m <sup>6</sup> A	N <sup>6</sup> -methyl-adenosine
METTL3	methyltransferase-like 3
METTL14	methyltransferase-like 14
WTAP	Wilms' tumor 1-associated protein
FTO	fat-mass and obesity-associated protein
ALKBH5	α-ketoglutarate-dependent dioxygenase alkB homolog 5
VEGF	vascular endothelial growth factor
ESCs	embryonic stem cells

## References

- Amort, T.; Rieder, D.; Wille, A.; Khokhlova-Cubberley, D.; Riml, C.; Trixl, L.; Jia, X.Y.; Micura, R.; Lusser, A. Distinct 5-methylcytosine profiles in poly(A) RNA from mouse embryonic stem cells and brain. *Genome Biol.* **2017**, *18*, 1. [[CrossRef](#)] [[PubMed](#)]
- Zhou, Y.; Zeng, P.; Li, Y.H.; Zhang, Z.; Cui, Q. SRAMP: Prediction of mammalian N<sup>6</sup>-methyladenosine (m<sup>6</sup>A) sites based on sequence-derived features. *Nucleic Acids Res.* **2016**, *44*, e91. [[CrossRef](#)] [[PubMed](#)]
- Dominissini, D.; Moshitch-Moshkovitz, S.; Schwartz, S.; Salmon-Divon, M.; Ungar, L.; Osenberg, S.; Cesarkas, K.; Jacob-Hirsch, J.; Amariglio, N.; Kupiec, M.; et al. Topology of the human and mouse m<sup>6</sup>A RNA methylomes revealed by m<sup>6</sup>A-seq. *Nature* **2012**, *485*, 201–206. [[CrossRef](#)] [[PubMed](#)]
- Zheng, Y.; Nie, P.; Peng, D.; He, Z.; Liu, M.; Xie, Y.; Miao, Y.; Zuo, Z.; Ren, J. m<sup>6</sup>AVar: A database of functional variants involved in m<sup>6</sup>A modification. *Nucleic Acids Res.* **2018**, *46*, D139–D145. [[CrossRef](#)] [[PubMed](#)]
- Liu, Z.; Zhang, J. Most m<sup>6</sup>A RNA modifications in protein-coding regions are evolutionarily unconserved and likely nonfunctional. *Mol. Biol. Evol.* **2017**, *35*, 666–675. [[CrossRef](#)] [[PubMed](#)]
- Schwartz, S.; Mumbach, M.R.; Jovanovic, M.; Wang, T.; Maciag, K.; Bushkin, G.G.; Mertins, P.; Ter-Ovanesyan, D.; Habib, N.; Cacchiarelli, D.; et al. Perturbation of m<sup>6</sup>A writers reveals two distinct classes of mRNA methylation at internal and 5' sites. *Cell Rep.* **2014**, *8*, 284–296. [[CrossRef](#)] [[PubMed](#)]
- Wang, P.; Doxtader, K.A.; Nam, Y. Structural Basis for Cooperative Function of Mettl3 and Mettl14 Methyltransferases. *Mol. Cell* **2016**, *63*, 306–317. [[CrossRef](#)]
- Punekar, A.S.; Liljeruhm, J.; Shepherd, T.R.; Forster, A.C.; Selmer, M. Structural and functional insights into the molecular mechanism of rRNA m<sup>6</sup>A methyltransferase RlmJ. *Nucleic Acids Res.* **2013**, *41*, 9537–9548. [[CrossRef](#)]
- Zhang, C.; Samanta, D.; Lu, H.; Bullen, J.W.; Zhang, H.; Chen, I.; He, X.; Semenza, G.L. Hypoxia induces the breast cancer stem cell phenotype by HIF-dependent and ALKBH5-mediated m(6)A-demethylation of NANOG mRNA. *Proc. Natl. Acad. Sci. USA.* **2016**, *113*, E2047–E2056. [[CrossRef](#)]
- Jia, G.; Fu, Y.; He, C. Reversible RNA adenosine methylation in biological regulation. *Trends Genet.* **2013**, *29*, 108–115. [[CrossRef](#)]
- Wang, X.; Lu, Z.; Gomez, A.; Hon, G.C.; Yue, Y.; Han, D.; Fu, Y.; Parisien, M.; Dai, Q.; Jia, G.; et al. N<sup>6</sup>-methyladenosine-dependent regulation of messenger RNA stability. *Nature* **2014**, *505*, 117–120. [[CrossRef](#)] [[PubMed](#)]
- Liu, N.; Dai, Q.; Zheng, G.; He, C.; Parisien, M.; Pan, T. N(6)-methyladenosine-dependent RNA structural switches regulate RNA-protein interactions. *Nature* **2015**, *518*, 560–564. [[CrossRef](#)] [[PubMed](#)]
- Maity, A.; Das, B. N<sup>6</sup>-methyladenosine modification in mRNA: Machinery, function and implications for health and diseases. *FEBS J.* **2016**, *283*, 1607–1630. [[CrossRef](#)] [[PubMed](#)]
- Cui, Q.; Shi, H.; Ye, P.; Li, L.; Qu, Q.; Sun, G.; Sun, G.; Lu, Z.; Huang, Y.; Yang, C.G.; et al. m(6)A RNA methylation regulates the self-renewal and tumorigenesis of glioblastoma stem cells. *Cell Rep.* **2017**, *18*, 2622–2634. [[CrossRef](#)] [[PubMed](#)]
- Zhao, B.S.; Roundtree, I.A.; He, C. Post-transcriptional gene regulation by mRNA modifications. *Nat. Rev. Mol. Cell Biol.* **2017**, *18*, 31–42. [[CrossRef](#)] [[PubMed](#)]
- Macrin, D.; Joseph, J.P.; Pillai, A.A.; Devi, A. Eminent sources of adult mesenchymal stem cells and their therapeutic imminence. *Stem Cell Rev.* **2017**, *13*, 741–756. [[CrossRef](#)] [[PubMed](#)]

17. Kadekar, D.; Kale, V.; Limaye, L. Differential ability of MSCs isolated from placenta and cord as feeders for supporting ex vivo expansion of umbilical cord blood derived CD34(+) cells. *Stem Cell Res. Ther.* **2015**, *6*, 201. [[CrossRef](#)]
18. Xu, Y.; Li, Z.; Li, X.; Fan, Z.; Liu, Z.; Xie, X.; Guan, J. Regulating myogenic differentiation of mesenchymal stem cells using thermosensitive hydrogels. *Acta Biomater.* **2015**, *26*, 23–33. [[CrossRef](#)]
19. Li, Q.; Gao, Z.; Chen, Y.; Guan, M.X. The role of mitochondria in osteogenic, adipogenic and chondrogenic differentiation of mesenchymal stem cells. *Protein Cell* **2017**, *8*, 439–445. [[CrossRef](#)]
20. Van Zoelen, E.J.; Duarte, I.; Hendriks, J.M.; van der Woning, S.P. TGFbeta-induced switch from adipogenic to osteogenic differentiation of human mesenchymal stem cells: Identification of drug targets for prevention of fat cell differentiation. *Stem Cell Res. Ther.* **2016**, *7*, 123. [[CrossRef](#)]
21. Dzobo, K.; Vogelsang, M.; Thomford, N.E.; Dandara, C.; Kallmeyer, K.; Pepper, M.S.; Parker, M.I. Wharton's Jelly-derived mesenchymal stromal cells and fibroblast-derived extracellular matrix synergistically activate apoptosis in a p21-dependent mechanism in WHCO1 and MDA MB 231 cancer cells in vitro. *Stem Cells Int.* **2016**, *2016*, 4842134. [[CrossRef](#)] [[PubMed](#)]
22. Dzobo, K.; Turnley, T.; Wishart, A.; Rowe, A.; Kallmeyer, K.; van Vollenstee, F.A.; Thomford, N.E.; Dandara, C.; Chopera, D.; Pepper, M.S.; et al. Fibroblast-derived extracellular matrix induces chondrogenic differentiation in human adipose-derived mesenchymal stromal/stem cells in Vitro. *Int. J. Mol. Sci.* **2016**, *17*, 1259. [[CrossRef](#)] [[PubMed](#)]
23. Tu, C.; Xiao, Y.; Ma, Y.; Wu, H.; Song, M. The legacy effects of electromagnetic fields on bone marrow mesenchymal stem cell self-renewal and multiple differentiation potential. *Stem Cell Res. Ther.* **2018**, *9*, 215. [[CrossRef](#)] [[PubMed](#)]
24. Waldner, M.; Zhang, W.; James, I.B.; Allbright, K.; Havis, E.; Bliley, J.M.; Almadori, A.; Schweizer, R.; Plock, J.A.; Washington, K.M.; et al. Characteristics and immunomodulating functions of adipose-derived and bone marrow-derived mesenchymal stem cells across defined human leukocyte antigen barriers. *Front. Immunol.* **2018**, *9*, 1642. [[CrossRef](#)] [[PubMed](#)]
25. Dzobo, K.; Thomford, N.E.; Senthebane, D.A.; Shipanga, H.; Rowe, A.; Dandara, C.; Pillay, M.; Motaung, K. Advances in Regenerative Medicine and Tissue Engineering: Innovation and Transformation of Medicine. *Stem Cells Int.* **2018**, *2018*, 2495848. [[CrossRef](#)] [[PubMed](#)]
26. Liao, L.; Shi, B.; Chang, H.; Su, X.; Zhang, L.; Bi, C.; Shuai, Y.; Du, X.; Deng, Z.; Jin, Y. Heparin improves BMSC cell therapy: Anticoagulant treatment by heparin improves the safety and therapeutic effect of bone marrow-derived mesenchymal stem cell cytotераpy. *Theranostics* **2017**, *7*, 106–116. [[CrossRef](#)] [[PubMed](#)]
27. Forostyak, S.; Jendelova, P.; Sykova, E. The role of mesenchymal stromal cells in spinal cord injury, regenerative medicine and possible clinical applications. *Biochimie* **2013**, *95*, 2257–2270. [[CrossRef](#)]
28. Vaquero, J.; Zurita, M. Functional recovery after severe CNS trauma: Current perspectives for cell therapy with bone marrow stromal cells. *Prog. Neurobiol.* **2011**, *93*, 341–349. [[CrossRef](#)] [[PubMed](#)]
29. Tsai, T.L.; Li, W.J. Identification of bone marrow-derived soluble factors regulating human mesenchymal stem cells for bone regeneration. *Stem Cell Rep.* **2017**, *8*, 387–400. [[CrossRef](#)] [[PubMed](#)]
30. Shu, Y.; Yu, Y.; Zhang, S.; Wang, J.; Xiao, Y.; Liu, C. The immunomodulatory role of sulfated chitosan in BMP-2-mediated bone regeneration. *Biomater. Sci.* **2018**, *6*, 2496–2507. [[CrossRef](#)]
31. Hu, K.; Olsen, B.R. The roles of vascular endothelial growth factor in bone repair and regeneration. *Bone* **2016**, *91*, 30–38. [[CrossRef](#)] [[PubMed](#)]
32. Liu, X.; Bao, C.; Xu, H.; Pan, J.; Hu, J.; Wang, P.; Luo, E. Osteoprotegerin gene-modified BMSCs with hydroxyapatite scaffold for treating critical-sized mandibular defects in ovariectomized osteoporotic rats. *Acta Biomater.* **2016**, *42*, 378–388. [[CrossRef](#)] [[PubMed](#)]
33. Hankenson, K.D.; Gagne, K.; Shaughnessy, M. Extracellular signaling molecules to promote fracture healing and bone regeneration. *Adv. Drug Deliv. Rev.* **2015**, *94*, 3–12. [[CrossRef](#)] [[PubMed](#)]
34. Stegen, S.; van Gestel, N.; Carmeliet, G. Bringing new life to damaged bone: The importance of angiogenesis in bone repair and regeneration. *Bone* **2015**, *70*, 19–27. [[CrossRef](#)] [[PubMed](#)]
35. Montespan, F.; Deschaseaux, F.; Sensebe, L.; Carosella, E.D.; Rouas-Freiss, N. Osteodifferentiated mesenchymal stem cells from bone marrow and adipose tissue express HLA-G and display immunomodulatory properties in HLA-mismatched settings: Implications in bone repair therapy. *J. Immunol. Res.* **2014**, *2014*, 230346. [[CrossRef](#)] [[PubMed](#)]

36. Zhang, L.; Tang, Y.; Zhu, X.; Tu, T.; Sui, L.; Han, Q.; Yu, L.; Meng, S.; Zheng, L.; Valverde, P.; et al. Overexpression of MiR-335-5p Promotes Bone Formation and Regeneration in Mice. *J. Bone Miner. Res.* **2017**, *32*, 2466–2475. [[CrossRef](#)] [[PubMed](#)]
37. Cipitria, A.; Boettcher, K.; Schoenhals, S.; Garske, D.S.; Schmidt-Bleek, K.; Ellinghaus, A.; Dienelt, A.; Peters, A.; Mehta, M.; Madl, C.M.; et al. In-situ tissue regeneration through SDF-1alpha driven cell recruitment and stiffness-mediated bone regeneration in a critical-sized segmental femoral defect. *Acta Biomater.* **2017**, *60*, 50–63. [[CrossRef](#)] [[PubMed](#)]
38. Yan, P.; Xia, C.; Duan, C.; Li, S.; Mei, Z. Biological characteristics of foam cell formation in smooth muscle cells derived from bone marrow stem cells. *Int. J. Biol. Sci.* **2011**, *7*, 937–946. [[CrossRef](#)] [[PubMed](#)]
39. Hu, B.; Li, Y.; Wang, M.; Zhu, Y.; Zhou, Y.; Sui, B.; Tan, Y.; Ning, Y.; Wang, J.; He, J.; et al. Functional reconstruction of critical-sized load-bearing bone defects using a Sclerostin-targeting miR-210-3p-based construct to enhance osteogenic activity. *Acta Biomater.* **2018**, *76*, 275–282. [[CrossRef](#)] [[PubMed](#)]
40. Kang, M.L.; Kim, J.E.; Im, G.I. Vascular endothelial growth factor-transfected adipose-derived stromal cells enhance bone regeneration and neovascularization from bone marrow stromal cells. *J. Tissue Eng. Regen. Med.* **2017**, *11*, 3337–3348. [[CrossRef](#)]
41. Qiu, G.; Shi, Z.; Xu, H.; Yang, B.; Weir, M.D.; Li, G.; Song, Y.; Wang, J.; Hu, K.; Wang, P.; et al. Bone regeneration in minipigs via calcium phosphate cement scaffold delivering autologous bone marrow mesenchymal stem cells and platelet-rich plasma. *J. Tissue Eng. Regen. Med.* **2018**, *12*, e937–e948. [[CrossRef](#)] [[PubMed](#)]
42. Wu, X.; Wang, Q.; Kang, N.; Wu, J.; Gu, C.; Bi, J.; Lv, T.; Xie, F.; Hu, J.; Liu, X.; et al. The effects of different vascular carrier patterns on the angiogenesis and osteogenesis of BMSC-TCP-based tissue-engineered bone in beagle dogs. *J. Tissue Eng. Regen. Med.* **2017**, *11*, 542–552. [[CrossRef](#)] [[PubMed](#)]
43. Wang, R.; Xu, B.; Xu, H.G. Up-regulation of TGF-beta promotes tendon-to-bone healing after anterior cruciate ligament reconstruction using bone marrow-derived mesenchymal stem cells through the TGF-beta/MAPK signaling pathway in a new zealand white rabbit model. *Cell. Physiol. Biochem.* **2017**, *41*, 213–226. [[CrossRef](#)] [[PubMed](#)]
44. Kuttapitiya, A.; Assi, L.; Laing, K.; Hing, C.; Mitchell, P.; Whitley, G.; Harrison, A.; Howe, F.A.; Ejindu, V.; Heron, C.; et al. Microarray analysis of bone marrow lesions in osteoarthritis demonstrates upregulation of genes implicated in osteochondral turnover, neurogenesis and inflammation. *Ann. Rheum. Dis.* **2017**, *76*, 1764–1773. [[CrossRef](#)] [[PubMed](#)]
45. Chimutengwende-Gordon, M.; Mbogo, A.; Khan, W.; Wilkes, R. Limb reconstruction after traumatic bone loss. *Injury* **2017**, *48*, 206–213. [[CrossRef](#)]
46. Emori, M.; Kaya, M.; Irifune, H.; Takahashi, N.; Shimizu, J.; Mizushima, E.; Murahashi, Y.; Yamashita, T. Vascularised fibular grafts for reconstruction of extremity bone defects after resection of bone and soft-tissue tumours: A single institutional study of 49 patients. *Bone Joint J.* **2017**, *99*, 1237–1243. [[CrossRef](#)] [[PubMed](#)]
47. Huang, R.L.; Sun, Y.; Ho, C.K.; Liu, K.; Tang, Q.Q.; Xie, Y.; Li, Q. IL-6 potentiates BMP-2-induced osteogenesis and adipogenesis via two different BMPRI1A-mediated pathways. *Cell Death Dis.* **2018**, *9*, 144. [[CrossRef](#)] [[PubMed](#)]
48. Zhang, W.B.; Zhong, W.J.; Wang, L. A signal-amplification circuit between miR-218 and Wnt/beta-catenin signal promotes human adipose tissue-derived stem cells osteogenic differentiation. *Bone* **2014**, *58*, 59–66. [[CrossRef](#)]
49. Meng, J.; Ma, X.; Wang, N.; Jia, M.; Bi, L.; Wang, Y.; Li, M.; Zhang, H.; Xue, X.; Hou, Z.; et al. Activation of GLP-1 receptor promotes bone marrow stromal cell osteogenic differentiation through beta-Catenin. *Stem Cell Rep.* **2016**, *6*, 579–591. [[CrossRef](#)] [[PubMed](#)]
50. Jiao, X.; Cai, J.; Yu, X.; Ding, X. Paracrine activation of the Wnt/beta-catenin pathway by bone marrow stem cell attenuates cisplatin-induced kidney injury. *Cell. Physiol. Biochem.* **2017**, *44*, 1980–1994. [[CrossRef](#)] [[PubMed](#)]
51. Wen, Q.; Zhang, S.; Du, X.; Wang, R.; Li, Y.; Liu, H.; Hu, S.; Zhou, C.; Zhou, X.; Ma, L. The multiplicity of infection-dependent effects of recombinant adenovirus carrying HGF gene on the proliferation and osteogenic differentiation of human bone marrow mesenchymal stem cells. *Int. J. Mol. Sci.* **2018**, *19*, 734.
52. Ramasamy, S.K.; Kusumbe, A.P.; Wang, L.; Adams, R.H. Endothelial Notch activity promotes angiogenesis and osteogenesis in bone. *Nature* **2014**, *507*, 376–380. [[CrossRef](#)]

53. Mao, L.; Xia, L.; Chang, J.; Liu, J.; Jiang, L.; Wu, C.; Fang, B. The synergistic effects of Sr and Si bioactive ions on osteogenesis, osteoclastogenesis and angiogenesis for osteoporotic bone regeneration. *Acta Biomater.* **2017**, *61*, 217–232. [[CrossRef](#)] [[PubMed](#)]
54. Huang, C.; Ness, V.P.; Yang, X.; Chen, H.; Luo, J.; Brown, E.B.; Zhang, X. Spatiotemporal analyses of osteogenesis and angiogenesis via intravital imaging in cranial bone defect repair. *J. Bone Miner. Res.* **2015**, *30*, 1217–1230. [[CrossRef](#)]
55. Busilacchi, A.; Gigante, A.; Mattioli-Belmonte, M.; Manzotti, S.; Muzzarelli, R.A. Chitosan stabilizes platelet growth factors and modulates stem cell differentiation toward tissue regeneration. *Carbohydr. Polym.* **2013**, *98*, 665–676. [[CrossRef](#)] [[PubMed](#)]
56. Hu, K.; Olsen, B.R. Osteoblast-derived VEGF regulates osteoblast differentiation and bone formation during bone repair. *J. Clin. Investig.* **2016**, *126*, 509–526. [[CrossRef](#)] [[PubMed](#)]
57. Li, B.; Wang, H.; Qiu, G.; Su, X.; Wu, Z. Synergistic Effects of vascular endothelial growth factor on bone morphogenetic proteins induced bone formation in Vivo: Influencing factors and future research directions. *Biomed Res. Int.* **2016**, *2016*, 2869572. [[CrossRef](#)] [[PubMed](#)]
58. Kim, B.S.; Yang, S.S.; You, H.K.; Shin, H.I.; Lee, J. Fucoidan-induced osteogenic differentiation promotes angiogenesis by inducing vascular endothelial growth factor secretion and accelerates bone repair. *J. Tissue Eng. Regen. Med.* **2018**, *12*, e1311–e1324. [[CrossRef](#)] [[PubMed](#)]
59. Zhang, Y.; Ma, C.; Liu, X.; Wu, Z.; Yan, P.; Ma, N.; Fan, Q.; Zhao, Q. Epigenetic landscape in PPARgamma2 in the enhancement of adipogenesis of mouse osteoporotic bone marrow stromal cell. *Biochim. Biophys. Acta* **2015**, *1852*, 2504–2516. [[CrossRef](#)] [[PubMed](#)]
60. Lv, L.; Liu, Y.; Zhang, P.; Bai, X.; Ma, X.; Wang, Y.; Li, H.; Wang, L.; Zhou, Y. The epigenetic mechanisms of nanotopography-guided osteogenic differentiation of mesenchymal stem cells via high-throughput transcriptome sequencing. *Int. J. Nanomed.* **2018**, *13*, 5605–5623. [[CrossRef](#)] [[PubMed](#)]
61. Sepulveda, H.; Aguilar, R.; Prieto, C.P.; Bustos, F.; Aedo, S.; Lattus, J.; van Zundert, B.; Palma, V.; Montecino, M. Epigenetic signatures at the RUNX2-P1 and Sp7 gene promoters control osteogenic lineage commitment of umbilical cord-derived mesenchymal stem cells. *J. Cell. Physiol.* **2017**, *232*, 2519–2527. [[CrossRef](#)] [[PubMed](#)]
62. Cao, Y.; Yang, H.; Jin, L.; Du, J.; Fan, Z. Genome-Wide DNA Methylation analysis during osteogenic differentiation of human bone marrow mesenchymal stem cells. *Stem Cells Int.* **2018**, *2018*, 8238496. [[CrossRef](#)] [[PubMed](#)]
63. Jiang, S.; Xia, M.; Yang, J.; Shao, J.; Liao, X.; Zhu, J.; Jiang, H. Novel insights into a treatment for aplastic anemia based on the advanced proliferation of bone marrow-derived mesenchymal stem cells induced by fibroblast growth factor 1. *Mol. Med. Rep.* **2015**, *12*, 7877–7882. [[CrossRef](#)] [[PubMed](#)]
64. Yang, D.; Qiao, J.; Wang, G.; Lan, Y.; Li, G.; Guo, X.; Xi, J.; Ye, D.; Zhu, S.; Chen, W.; et al. N6-Methyladenosine modification of lincRNA 1281 is critically required for mESC differentiation potential. *Nucleic Acids Res.* **2018**, *46*, 3906–3920. [[CrossRef](#)] [[PubMed](#)]
65. Wang, Y.; Li, Y.; Yue, M.; Wang, J.; Kumar, S.; Wechsler-Reya, R.J.; Zhang, Z.; Ogawa, Y.; Kellis, M.; Duester, G.; et al. N(6)-methyladenosine RNA modification regulates embryonic neural stem cell self-renewal through histone modifications. *Nat. Neurosci.* **2018**, *21*, 195–206. [[CrossRef](#)] [[PubMed](#)]
66. Visvanathan, A.; Patil, V.; Arora, A.; Hegde, A.S.; Arivazhagan, A.; Santosh, V.; Somasundaram, K. Essential role of METTL3-mediated m(6)A modification in glioma stem-like cells maintenance and radioresistance. *Oncogene* **2018**, *37*, 522–533. [[CrossRef](#)]
67. Baralle, F.E.; Giudice, J. Alternative splicing as a regulator of development and tissue identity. *Nat. Rev. Mol. Cell Biol.* **2017**, *18*, 437–451. [[CrossRef](#)]
68. Naftelberg, S.; Schor, I.E.; Ast, G.; Kornblihtt, A.R. Regulation of alternative splicing through coupling with transcription and chromatin structure. *Annu. Rev. Biochem.* **2015**, *84*, 165–198. [[CrossRef](#)]
69. Feng, Z.; Li, Q.; Meng, R.; Yi, B.; Xu, Q. METTL3 regulates alternative splicing of MyD88 upon the lipopolysaccharide-induced inflammatory response in human dental pulp cells. *J. Cell. Mol. Med.* **2018**, *22*, 2558–2568. [[CrossRef](#)]
70. Xu, K.; Yang, Y.; Feng, G.H.; Sun, B.F.; Chen, J.Q.; Li, Y.F.; Chen, Y.S.; Zhang, X.X.; Wang, C.X.; Jiang, L.Y.; et al. Mettl3-mediated m(6)A regulates spermatogonial differentiation and meiosis initiation. *Cell Res.* **2017**, *27*, 1100–1114. [[CrossRef](#)]

71. Haussmann, I.U.; Bodi, Z.; Sanchez-Moran, E.; Mongan, N.P.; Archer, N.; Fray, R.G.; Soller, M. m(6)A potentiates Sxl alternative pre-mRNA splicing for robust *Drosophila* sex determination. *Nature* **2016**, *540*, 301–304. [[CrossRef](#)] [[PubMed](#)]
72. Lin, H.; Shabbir, A.; Molnar, M.; Yang, J.; Marion, S.; Canty, J.J.; Lee, T. Adenoviral expression of vascular endothelial growth factor splice variants differentially regulate bone marrow-derived mesenchymal stem cells. *J. Cell. Physiol.* **2008**, *216*, 458–468. [[CrossRef](#)] [[PubMed](#)]
73. Li, R.; Nauth, A.; Li, C.; Qamirani, E.; Atesok, K.; Schemitsch, E.H. Expression of VEGF gene isoforms in a rat segmental bone defect model treated with EPCs. *J. Orthop. Trauma.* **2012**, *26*, 689–692. [[CrossRef](#)] [[PubMed](#)]
74. Breier, G.; Albrecht, U.; Sterrer, S.; Risau, W. Expression of vascular endothelial growth factor during embryonic angiogenesis and endothelial cell differentiation. *Development* **1992**, *114*, 521–532. [[PubMed](#)]
75. Linder, B.; Grozhik, A.V.; Olarerin-George, A.O.; Meydan, C.; Mason, C.E.; Jaffrey, S.R. Single-nucleotide-resolution mapping of m6A and m6Am throughout the transcriptome. *Nat. Methods* **2015**, *12*, 767–772. [[CrossRef](#)] [[PubMed](#)]
76. Luo, G.Z.; MacQueen, A.; Zheng, G.; Duan, H.; Dore, L.C.; Lu, Z.; Liu, J.; Chen, K.; Jia, G.; Bergelson, J.; et al. Unique features of the m6A methylome in *Arabidopsis thaliana*. *Nat. Commun.* **2014**, *5*, 5630. [[CrossRef](#)]
77. Martínez-Pérez, M.; Aparicio, F.; López-Gresa, M.P.; Bellés, J.M.; Sánchez-Navarro, J.A.; Pallás, V. *Arabidopsis* m6A demethylase activity modulates viral infection of a plant virus and the m6A abundance in its genomic RNAs. *Proc. Natl. Acad. Sci. USA* **2017**, *114*, 10755–10760. [[CrossRef](#)]
78. Wang, Y.; Li, Y.; Toth, J.I.; Petroski, M.D.; Zhang, Z.; Zhao, J.C. N6-methyladenosine modification destabilizes developmental regulators in embryonic stem cells. *Nat. Cell Biol.* **2014**, *16*, 191–198. [[CrossRef](#)]
79. Geula, S.; Moshitch-Moshkovitz, S.; Dominissini, D.; Mansour, A.A.; Kol, N.; Salmon-Divon, M.; Hershkovitz, V.; Peer, E.; Mor, N.; Manor, Y.S.; et al. Stem cells. m6A mRNA methylation facilitates resolution of naive pluripotency toward differentiation. *Science* **2015**, *347*, 1002–1006. [[CrossRef](#)]
80. Chen, T.; Hao, Y.J.; Zhang, Y.; Li, M.M.; Wang, M.; Han, W.; Wu, Y.; Lv, Y.; Hao, J.; Wang, L.; et al. m(6)A RNA methylation is regulated by microRNAs and promotes reprogramming to pluripotency. *Cell Stem Cell* **2015**, *16*, 289–301. [[CrossRef](#)]
81. Wang, C.X.; Cui, G.S.; Liu, X.; Xu, K.; Wang, M.; Zhang, X.X.; Jiang, L.Y.; Li, A.; Yang, Y.; Lai, W.Y.; et al. METTL3-mediated m6A modification is required for cerebellar development. *PLoS Biol.* **2018**, *16*, e2004880. [[CrossRef](#)] [[PubMed](#)]
82. Barbieri, I.; Tzelepis, K.; Pandolfini, L.; Shi, J.; Millan-Zambrano, G.; Robson, S.C.; Aspris, D.; Migliori, V.; Bannister, A.J.; Han, N.; et al. Promoter-bound METTL3 maintains myeloid leukaemia by m(6)A-dependent translation control. *Nature* **2017**, *552*, 126–131. [[CrossRef](#)] [[PubMed](#)]
83. Ping, X.L.; Sun, B.F.; Wang, L.; Xiao, W.; Yang, X.; Wang, W.J.; Adhikari, S.; Shi, Y.; Lv, Y.; Chen, Y.S.; et al. Mammalian WTAP is a regulatory subunit of the RNA N6-methyladenosine methyltransferase. *Cell Res.* **2014**, *24*, 177–189. [[CrossRef](#)] [[PubMed](#)]
84. Batista, P.J.; Molinie, B.; Wang, J.; Qu, K.; Zhang, J.; Li, L.; Bouley, D.M.; Lujan, E.; Haddad, B.; Daneshvar, K.; et al. m(6)A RNA modification controls cell fate transition in mammalian embryonic stem cells. *Cell Stem Cell* **2014**, *15*, 707–719. [[CrossRef](#)]
85. Dominissini, D.; Moshitch-Moshkovitz, S.; Salmon-Divon, M.; Amariglio, N.; Rechavi, G. Transcriptome-wide mapping of N(6)-methyladenosine by m(6)A-seq based on immunocapturing and massively parallel sequencing. *Nat. Protoc.* **2013**, *8*, 176–189. [[CrossRef](#)] [[PubMed](#)]
86. Bodi, Z.; Zhong, S.; Mehra, S.; Song, J.; Graham, N.; Li, H.; May, S.; Fray, R.G. Adenosine methylation in *Arabidopsis* mRNA is associated with the 3' end and reduced levels cause developmental defects. *Front. Plant Sci.* **2012**, *3*, 48. [[CrossRef](#)]
87. Hongay, C.F.; Orr-Weaver, T.L. *Drosophila* Inducer of MEiosis 4 (IME4) is required for Notch signaling during oogenesis. *Proc. Natl. Acad. Sci. USA* **2011**, *108*, 14855–14860. [[CrossRef](#)] [[PubMed](#)]
88. Yue, Y.; Liu, J.; He, C. RNA N6-methyladenosine methylation in post-transcriptional gene expression regulation. *Genes Dev.* **2015**, *29*, 1343–1355. [[CrossRef](#)] [[PubMed](#)]
89. Tong, Y.; Feng, W.; Wu, Y.; Lv, H.; Jia, Y.; Jiang, D. Mechano-growth factor accelerates the proliferation and osteogenic differentiation of rabbit mesenchymal stem cells through the PI3K/AKT pathway. *BMC Biochem.* **2015**, *16*, 1. [[CrossRef](#)] [[PubMed](#)]

90. Baker, N.; Sohn, J.; Tuan, R.S. Promotion of human mesenchymal stem cell osteogenesis by PI3-kinase/Akt signaling, and the influence of caveolin-1/cholesterol homeostasis. *Stem Cell Res. Ther.* **2015**, *6*, 238. [[CrossRef](#)]
91. Marie, P.J. Signaling pathways affecting skeletal health. *Curr. Osteoporos. Rep.* **2012**, *10*, 190–198. [[CrossRef](#)] [[PubMed](#)]
92. Garcia, J.R.; Clark, A.Y.; Garcia, A.J. Integrin-specific hydrogels functionalized with VEGF for vascularization and bone regeneration of critical-size bone defects. *J. Biomed. Mater. Res.* **2016**, *104*, 889–900. [[CrossRef](#)] [[PubMed](#)]
93. Zigdon-Giladi, H.; Bick, T.; Lewinson, D.; Machtei, E.E. Mesenchymal stem cells and endothelial progenitor cells stimulate bone regeneration and mineral density. *J. Periodontol.* **2014**, *85*, 984–990. [[CrossRef](#)] [[PubMed](#)]
94. Kaner, D.; Zhao, H.; Terheyden, H.; Friedmann, A. Improvement of microcirculation and wound healing in vertical ridge augmentation after pre-treatment with self-inflating soft tissue expanders—A randomized study in dogs. *Clin. Oral Implants Res.* **2015**, *26*, 720–724. [[CrossRef](#)] [[PubMed](#)]
95. Duda, G.N.; Taylor, W.R.; Winkler, T.; Matziolis, G.; Heller, M.O.; Haas, N.P.; Perka, C.; Schaser, K.D. Biomechanical, microvascular, and cellular factors promote muscle and bone regeneration. *Exerc. Sport Sci. Rev.* **2008**, *36*, 64–70. [[CrossRef](#)] [[PubMed](#)]
96. Egri, S.; Eczacioglu, N. Sequential VEGF and BMP-2 releasing PLA-PEG-PLA scaffolds for bone tissue engineering: I. Design and in vitro tests. *Artif. Cells Nanomed. Biotechnol.* **2017**, *45*, 321–329. [[CrossRef](#)]
97. Pi, C.J.; Liang, K.L.; Ke, Z.Y.; Chen, F.; Cheng, Y.; Yin, L.J.; Deng, Z.L.; He, B.C.; Chen, L. Adenovirus-mediated expression of vascular endothelial growth factor- $\alpha$  potentiates bone morphogenetic protein-9-induced osteogenic differentiation and bone formation. *Biol. Chem.* **2016**, *397*, 765–775. [[CrossRef](#)] [[PubMed](#)]
98. Khojasteh, A.; Fahimipour, F.; Eslaminejad, M.B.; Jafarian, M.; Jahangir, S.; Bastami, F.; Tahriri, M.; Karkhaneh, A.; Tayebi, L. Development of PLGA-coated beta-TCP scaffolds containing VEGF for bone tissue engineering. *Mater. Sci. Eng. C Mater. Biol. Appl.* **2016**, *69*, 780–788. [[CrossRef](#)] [[PubMed](#)]
99. Carmeliet, P.; Ng, Y.S.; Nuyens, D.; Theilmeier, G.; Brusselmans, K.; Cornelissen, I.; Ehler, E.; Kakkar, V.V.; Stalmans, I.; Mattot, V.; et al. Impaired myocardial angiogenesis and ischemic cardiomyopathy in mice lacking the vascular endothelial growth factor isoforms VEGF164 and VEGF188. *Nat. Med.* **1999**, *5*, 495–502. [[CrossRef](#)] [[PubMed](#)]
100. Ke, S.; Pandya-Jones, A.; Saito, Y.; Fak, J.J.; Vagbo, C.B.; Geula, S.; Hanna, J.H.; Black, D.L.; Darnell, J.J.; Darnell, R.B. m(6)A mRNA modifications are deposited in nascent pre-mRNA and are not required for splicing but do specify cytoplasmic turnover. *Genes Dev.* **2017**, *31*, 990–1006. [[CrossRef](#)] [[PubMed](#)]
101. Liu, Y.; Ming, L.; Luo, H.; Liu, W.; Zhang, Y.; Liu, H.; Jin, Y. Integration of a calcined bovine bone and BMSC-sheet 3D scaffold and the promotion of bone regeneration in large defects. *Biomaterials* **2013**, *34*, 9998–10006. [[CrossRef](#)] [[PubMed](#)]
102. Li, R.; Li, C.H.; Nauth, A.; McKee, M.D.; Schemitsch, E.H. Effect of human vascular endothelial growth factor gene transfer on endogenous vascular endothelial growth factor mRNA expression in a rat fibroblast and osteoblast culture model. *J. Orthop. Trauma* **2010**, *24*, 547–551. [[CrossRef](#)] [[PubMed](#)]

